PCCP

Dynamic Article Links

Cite this: *Phys. Chem. Chem. Phys.*, 2011, **13**, 18347–18354

www.rsc.org/pccp

PAPER

Microsolvation of Co^{2+} and Ni^{2+} by acetonitrile and water: photodissociation dynamics of $M^{2+}(CH_3CN)_n(H_2O)_m$

Manori Perera,† Paul Ganssle and Ricardo B. Metz*

Received 16th May 2011, Accepted 17th August 2011
DOI: 10.1039/c1cp21586h

The microsolvation of cobalt and nickel dications by acetonitrile and water is studied by measuring photofragment spectra at 355, 532 and 560–660 nm. Ions are produced by electrospray, thermalized in an ion trap and mass selected by time of flight. The photodissociation yield, products and their branching ratios depend on the metal, cluster size and composition. Proton transfer is only observed in water-containing clusters and is enhanced with increasing water content. Also, nickel-containing clusters are more likely to undergo charge reduction than those with cobalt. The homogeneous clusters with acetonitrile $M^{2+}(CH_3CN)_n$ (n = 3 and 4) dissociate by simple solvent loss; n = 2 clusters dissociate by electron transfer. Mixed acetonitrile/water clusters display more interesting dissociation dynamics. Again, larger clusters (n = 3 and 4) show simple solvent loss. Water loss is substantially favored over acetonitrile loss, which is understandable because acetonitrile is a stronger ligand due to its higher dipole moment and polarizability. Proton transfer, forming $H^+(CH_3CN)$, is observed as a minor channel for $M^{2+}(CH_3CN)_2(H_2O)_2$ and $M^{2+}(CH_3CN)_2(H_2O)$ but is not seen in $M^{2+}(CH_3CN)_3(H_2O)$. Studies of deuterated clusters confirm that water acts as the proton donor. We previously observed proton loss as the major channel for photolysis of $M^{2+}(H_2O)_4$. Measurements of the photodissociation yield reveal that four-coordinate Co^{2+} clusters dissociate more readily than Ni^{2+} clusters whereas for the three-coordinate clusters, dissociation is more efficient for Ni^{2+} clusters. For the two-coordinate clusters, dissociation is *via* electron transfer and the yield is low for both metals. Calculations of reaction energetics, dissociation barriers, and the positions of excited electronic states complement the experimental work. Proton transfer in photolysis of $Co^{2+}(CH_3CN)_2(H_2O)$ is calculated to occur *via* a $(CH_3CN)Co^{2+}$–OH^-–$H^+(NCCH_3)$ salt-bridge transition state, reducing kinetic energy release in the dissociation.

Introduction

Interactions of transition metal ions with solvent molecules are vital to many chemical and biological processes. Binding of ligands and solvent molecules to transition metals is crucial for proper functioning of metalloenzymes, and is key to homogeneous organometallic catalysis. These applications underscore the importance of understanding the interactions of solvent molecules with transition metal ions. In solution, transition metals are typically multiply charged species such as M^{2+} and M^{3+} because the charge on the metal is highly stabilized by the solvent molecules. Transition metal cations have a strong attraction to solvent molecules, due to their partially filled d-orbitals and characteristic multiple charges. In solution, one only has very limited control over the coordination number. In contrast, gas-phase clusters can be produced with a specific number of solvent molecules. This is critical to studying how the number and type of solvent molecules affect the stability and structure of the cluster. This has prompted numerous gas-phase studies, as evidenced by this special issue and several recent reviews.[1–3]

The preferred coordination number for metal ions such as Co^{2+} and Ni^{2+} with water is six, as in solution, but gas-phase clusters with fewer water molecules are readily produced.[4,5] Collision-induced dissociation (CID) of larger clusters leads to simple solvent loss. Smaller clusters dissociate by proton transfer, producing two singly charged ions: H_3O^+ and $MOH^+(H_2O)_m$. This is also observed in photodissociation studies of $Ni^{2+}(H_2O)_n$ and $Co^{2+}(H_2O)_n$, where proton transfer dominates for n = 4.[6–8] Proton transfer is less favorable for aprotic solvents such as acetonitrile. In addition, acetonitrile interacts more strongly with ions than does water due to its higher polarizability (4.40 *vs.* 1.45 Å^2) and dipole moment (3.92 *vs.* 1.85 D). As a result, small acetonitrile-containing

Department of Chemistry, University of Massachusetts Amherst, Amherst, MA 01003, USA. E-mail: rbmetz@chem.umass.edu; Fax: +1 4135454490; Tel: +1 4135456089
† Current address: Department of Chemistry, Illinois Wesleyan University, 201 E. Beecher St., Bloomington, IL 61702, USA.

clusters are more readily produced and studied. CID studies of $M^{2+}(CH_3CN)_n$ clusters reveal a rich assortment of dissociation pathways:[9–18]

$$M^{2+}(CH_3CN)_n \rightarrow \begin{cases} M^{2+}(CH_3CN)_{n-1} + CH_3CN & \text{solvent loss} \quad (1a) \\ M^{+}(CH_3CN)_{n-1} + CH_3CN^{+} & \text{electron transfer} \quad (1b) \\ [M(CH_2CN)]^{+}(CH_3CN)_{n-2} + H^{+}(CH_3CN) & \text{proton transfer} \quad (1c) \\ [MCN]^{+}(CH_3CN)_{n-1} + CH_3^{+} & \text{heterolytic bond cleavage} \quad (1d) \end{cases}$$

Solvent loss dominates for larger clusters, while electron transfer is usually favored for small clusters. However, the dissociation pathways depend on the metal, coordination number, and even on the collision energy. This has also been investigated in computational studies of the dissociation pathways of $M^{2+}(CH_3CN)_n$, $n = 1, 2$.[19]

Photoexcitation of the molecules provides better control over the available energy than CID studies. Our previous studies of the photodissociation dynamics and spectroscopy of $M^{2+}(L)_n$ (M = Co, Ni; L = H_2O[6,7] and CH_3OH[8]) involved excitation of metal-centered d–d transitions in the visible. These transitions are symmetry forbidden and thus tend to be weak. After absorbing a photon, the electronically excited molecules undergo internal conversion. The resulting highly vibrationally excited ground electronic state molecules can then dissociate. Guan *et al*. studied photolysis of $Ag^{2+}(L)_n$ complexes with several ligands in the visible and near-IR.[20] They observed photodissociation for complexes with ligands with low ionization energies, such as pyridine, and assign the transitions to ligand-to-metal charge transfer. They observed no photodissociation for acetonitrile complexes, which is not surprising, as the ionization energy of acetonitrile, 12.19 eV, is almost as high as that of water, 12.61 eV. Posey and coworkers also observed intense metal-to-ligand charge transfer transitions in solvated $M^{2+}(bipyridine)_3$ and related complexes.[21–23] In addition, there have been several studies of the vibrational spectroscopy of transition metal dication–water complexes. Duncan and co-workers measured the O–H stretches of $M^{2+}(H_2O)$ (M = Sc, Cr). Binding to the metal lowers the O–H stretching frequencies, and this effect is more pronounced for the dication than for the singly charged ion.[24,25] Williams, Saykally and co-workers have studied the vibrational spectroscopy of large $M^{2+}(H_2O)_n$ clusters (M = Mg,[26] Ca,[26–28] Ba,[26] Cu[29] and Zn[30]) in the O–H stretching region, measuring the size of the primary solvation shell and evolution toward the solution spectrum with increasing cluster size.

It is not very common to find studies of mixed solvent systems, but these systems are ideal for understanding the competing interactions that result due to differences in physical properties of the solvents, such as dipole moment and polarizability. The dipole moment of methanol is slightly smaller than that of water, but its polarizability is twice as large. Thus, methanol is found to bind metal dications more strongly than water, as shown by the observation that for mixed methanol/water clusters of Mn^{2+}, the first solvent shell primarily consists of methanol.[31] The competitive binding can lead to surprising results. In mixed benzene/water clusters, Na^+ coordinates to water only, while K^+ has benzene and water in the inner solvent shell.[32]

In this paper, we will discuss the results of photofragmentation of Co^{2+} and Ni^{2+} microsolvated by pure acetonitrile and a mixture of acetonitrile and water. These results will be compared to previous work on pure water complexes. Studies of mixed acetonitrile/water clusters provide insight into protic–aprotic solvent competition for the metal, and to competing dissociation pathways.

Experimental and computational methods

The dual time-of-flight photofragment mass spectrometer used in this study is described in detail in a review.[1] In this study, cluster ions are produced using electrospray with a 10^{-3}–10^{-4} M solution of the appropriate metal salt, $Co(NO_3)_2$ or $Ni(NO_3)_2$. It is essential to use nitrate salts as chlorides and sulfates do not dissolve sufficiently in acetonitrile. To control the water content, the salts were dried overnight under vacuum and the acetonitrile solvent was dried using molecular sieves for at least 24 h. It is critical that the salts and acetonitrile be free of water in the production of homogeneous metal–acetonitrile clusters. For the mixed clusters, water was added to the solution. As a result of increasing water content, the ESI needle voltage was increased.

Ions are formed at atmospheric pressure and enter the source chamber through a capillary heated to 50–70 °C. They then travel through an ion funnel[33] before heading to the next low pressure chamber. The alternating plates of the ion funnel have phase-shifted 1 MHz radiofrequency (rf) and a DC gradient. Using this technique, we are able to significantly improve the ion beam intensity, thus allowing us to study the smaller clusters. Producing the smaller clusters requires very different instrument conditions than for the four-coordinate or larger clusters. For example, the pressure in the source chamber is increased from ~200 mTorr to ~400 mTorr by partially throttling the mechanical pumps, and a higher DC gradient on the ion funnel is required. The ion funnel focuses the ions through a differential pumping aperture into the second differential region where an octopole ion guide introduces the ions into an rf Paul ion trap. Ions are trapped for up to 45 ms and are thermalized to ~300 K by collisions with the helium trap gas. They are then extracted into a reflectron time-of-flight mass spectrometer. The mass-selected ions of interest are irradiated at the turning point of the reflectron by the output of a pulsed (20 Hz) Nd:YAG laser, or a Nd:YAG pumped dye laser. The fragment and parent ions are re-accelerated down the flight tube and detected by a dual micro-channel-plate detector and identified by their characteristic flight times. The resulting signal is amplified, collected on a digital oscilloscope and recorded using a LabView-based program.

Difference time-of-flight spectra are used to identify the fragment pathways at a given wavelength, and can also show effects due to kinetic energy release and slow photodissociation.

A home-built chopper wheel assists in producing a difference spectrum by allowing for the subtraction of laser-on spectra from laser-off mass spectra. The photodissociation work was conducted at visible and ultraviolet wavelengths. None of the clusters dissociate at 355 nm. Photolysis deeper in the ultraviolet region, at 266 nm, produces no obvious fragments, although there is substantial background from the photolysis laser at this wavelength. In the visible, studies were carried out at 532 nm and at several wavelengths from 560 to 660 nm. Although the photodissociation yield depends on the visible wavelength, the observed products and dynamics do not show any obvious variability.

Calculations to complement the experimental work were initially conducted using B3LYP hybrid density functional theory with the 6-311+G basis set using *Gaussian 03*.[34] For each complex, the geometry was optimized and harmonic vibrational frequencies calculated to confirm the structure is a minimum (or, for transition states, a first-order saddle point). Subsequently, energies were calculated at the B3LYP/6-311++G(2df,2pd)//B3LYP/6-311+G level. This consists of a single-point energy calculation with the larger basis set, at the 6-311+G geometry. Calculated energies include the zero point energy (with the 6-311+G basis set) and thus correspond to 0 Kelvin values. In order to assess the accuracy of this hybrid calculation, the exothermicity and barrier of the $Co^{2+}(CH_3CN)_2(H_2O) \rightarrow CoOH^+(CH_3CN) + H^+(CH_3CN)$ reaction were also calculated completely at the B3LYP/6-311++G(2df,2pd) level. The results were very similar, with the B3LYP/6-311++G(2df,2pd) calculation increasing the exothermicity by 0.011 eV and decreasing the barrier by 0.007 eV, compared to the hybrid calculation.

Results and discussion

Microsolvation of Co^{2+} and Ni^{2+} by acetonitrile and water was studied specifically to understand (1) the interaction of solvents with the metal ion and (2) the competition between two different solvent molecules such as protic water and aprotic acetonitrile.

The mass spectra that were taken to identify the species present in the ion beam show a smooth cluster distribution from $n = 2$ to 5, with no pronounced "magic number" with unusually high intensity as shown in Fig. 1. Other studies[18] have shown that, under certain source conditions, acetonitrile-solvated metal ion clusters can have pronounced magic numbers, such as $Ni^{2+}(CH_3CN)_6$. The broader distribution we observe implies that our ion source is operating under harsher conditions. Previous work in our lab focused on protic solvents water and methanol.[6–8] During those studies the smallest cluster made in our lab was $M^{2+}(H_2O)_4$, but with acetonitrile we are able to make smaller clusters such as $M^{2+}(CH_3CN)_2$ because acetonitrile is a better solvent for M^{2+} due to its higher polarizability and dipole moment. Also, because acetonitrile is aprotic, it minimizes proton transfer dissociation in the ion source.

The fragment ions produced by photodissociation depend mainly on three factors: (1) whether the solvents in the cluster are homogenous or heterogeneous, (2) the coordination number of the cluster, and (3) the photon energy. Homologous $M^{2+}(CH_3CN)_n(H_2O)_m$ clusters for Co^{2+} and Ni^{2+} show very similar photodissociation dynamics but quite different yields. For simplicity, results will primarily be presented for cobalt clusters. Pathways are presented for 532 nm photolysis; the same channels are observed at 560–660 nm, with very similar branching ratios; no photolysis was observed at 355 nm.

A. Homogenous Co^{2+} and Ni^{2+} clusters with acetonitrile

Larger acetonitrile clusters $M^{2+}(CH_3CN)_n$, $n \geq 3$, dissociate exclusively by solvent loss. For $Co^{2+}(CH_3CN)_4$, the major dissociation channel is loss of one acetonitrile. Loss of two acetonitrile is a very minor channel for $Co^{2+}(CH_3CN)_4$ and is not observed for the nickel complex. The energetics for the observed dissociation pathways of $M^{2+}(CH_3CN)_n(H_2O)_m$ calculated at the B3LYP/6-311++G(2df,2pd)//B3LYP/6-311+G level for both metals are shown in Table 1. The energetics are similar for the two metals. Loss of one acetonitrile from $Co^{2+}(CH_3CN)_4$ is calculated to require 2.21 eV, which is near the laser photon energy at 532 nm (2.33 eV). The observed loss of two acetonitrile molecules is likely due to secondary photodissociation of the primary $Co^{2+}(CH_3CN)_3$ product. When mass-selected $Co^{2+}(CH_3CN)_3$ dissociates, the only product observed is simple loss of acetonitrile. The photodissociation yield for $Co^{2+}(CH_3CN)_3$ is much lower than for $Co^{2+}(CH_3CN)_4$. This is likely due to the much higher binding energy of the third solvent molecule (2.97 eV), which is significantly higher than the photon energy. Dissociation of these clusters is thus likely multiple-photon in nature. Solvent loss is the major photodissociation product of $Ni^{2+}(CH_3CN)_3$, but a small amount of electron transfer is also observed.

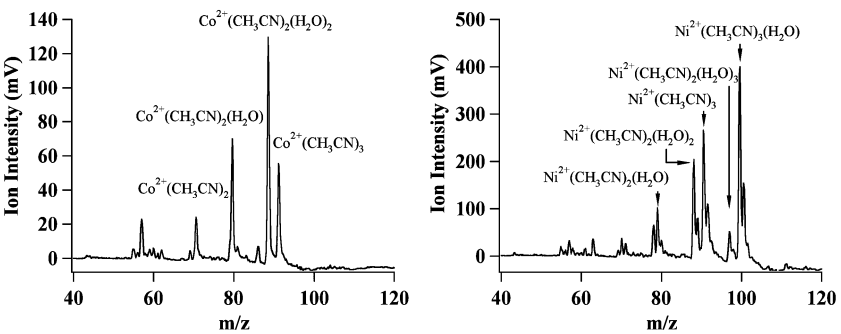

Fig. 1 Mass spectra of $Co^{2+}(CH_3CN)_n(H_2O)_m$ (left) and $Ni^{2+}(CH_3CN)_n(H_2O)_m$ clusters (right) formed by ESI of metal nitrate solutions in acetonitrile/water. The peaks in the nickel spectrum consist of doublets due to the two major $^{58}Ni^{2+}$ and $^{60}Ni^{2+}$ isotopes, which are separated by one m/z.

Table 1 Energies (in eV) for the dissociation reactions of $M^{2+}(CH_3CN)_n(H_2O)_m$ clusters calculated at the B3LYP/6-311++G(2df,2pd)//B3LYP/6-311+G level

Reaction	Co clusters	Ni clusters
Four-coordinate clusters		
$M^{2+}(CH_3CN)_4 \rightarrow M^{2+}(CH_3CN)_3 + CH_3CN$	2.21	2.14
$M^{2+}(CH_3CN)_4 \rightarrow M^{2+}(CH_3CN)_2 + 2CH_3CN$	5.18	5.02
$M^{2+}(CH_3CN)_3(H_2O) \rightarrow M^{2+}(CH_3CN)_3 + H_2O$	1.40	1.33
$M^{2+}(CH_3CN)_3(H_2O) \rightarrow M^{2+}(CH_3CN)_2(H_2O) + CH_3CN$	2.44	2.45
$M^{2+}(CH_3CN)_2(H_2O)_2 \rightarrow M^{2+}(CH_3CN)_2(H_2O) + H_2O$	1.50	1.50
$M^{2+}(CH_3CN)_2(H_2O)_2 \rightarrow M^{2+}(CH_3CN)(H_2O)_2 + CH_3CN$	2.65	2.59
Three-coordinate clusters		
$M^{2+}(CH_3CN)_3 \rightarrow M^{2+}(CH_3CN)_2 + CH_3CN$	2.97	2.88
$M^{2+}(CH_3CN)_2(H_2O) \rightarrow M^{2+}(CH_3CN)_2 + H_2O$	1.92	1.76
$M^{2+}(CH_3CN)_2(H_2O) \rightarrow M^{2+}(CH_3CN)(H_2O) + CH_3CN$	3.27	3.18
$M^{2+}(CH_3CN)_2(H_2O) \rightarrow MOH^{+}(CH_3CN) + H^{+}(CH_3CN)$	−0.53	−0.96
Two-coordinate clusters		
$M^{2+}(CH_3CN)_2 \rightarrow M^{+}(CH_3CN) + CH_3CN^{+}$	2.08	1.40
$M^{2+}(CH_3CN)_2 \rightarrow M^{2+}(CH_3CN) + CH_3CN$	4.42	4.59
$M^{2+}(CH_3CN)(H_2O) \rightarrow MOH^{+} + H^{+}(CH_3CN)$	−0.89	−1.09
$M^{2+}(CH_3CN)(H_2O) \rightarrow M^{2+}(CH_3CN) + H_2O$	3.08	3.17
$M^{2+}(CH_3CN)(H_2O) \rightarrow M^{2+}(H_2O) + CH_3CN$	4.96	5.20

The two-coordinate cluster, $Co^{2+}(CH_3CN)_2$, shows a new dissociation pathway: electron transfer to produce an acetonitrile cation, CH_3CN^{+}, and singly charged metal cation, $Co^{+}(CH_3CN)$, as shown in Fig. 2. In CID studies $M^{2+}(CH_3CN)_2$ exhibits proton transfer and electron transfer, but we only observe photodissociation *via* electron transfer. The electron and proton transfer products only differ by one mass unit, so there is the possibility that both pathways exist and the peaks overlap. To test this possibility, the study was extended using deuterated acetonitrile, CD_3CN. Deuteron transfer and electron transfer will result in fragments that are two mass units apart, making them easier to distinguish. The result shows only one fragment pathway: electron transfer. As with the three-coordinate clusters, the photofragment yield is very low. For $Co^{2+}(CH_3CN)_2$, electron transfer is energetically favored over solvent loss by 2.34 eV as shown in Table 1. Electron transfer is even more favorable for $Ni^{2+}(CH_3CN)_2$, due to its higher second ionization energy of 18.17 eV, as compared to 17.08 eV for cobalt. The very low photodissociation yield may be due to few molecules having sufficient energy to surmount the electron transfer activation barrier, or to low absorption cross section. The electron transfer fragment peaks show only slight broadening in the time-of-flight profile. This suggests that there is only very modest kinetic energy release in the dissociation, but it is hard to quantify, as the dissociation yield is so low. Unfortunately, we are not able to produce sufficient quantities of $M^{2+}(CH_3CN)$ to measure its photodissociation.

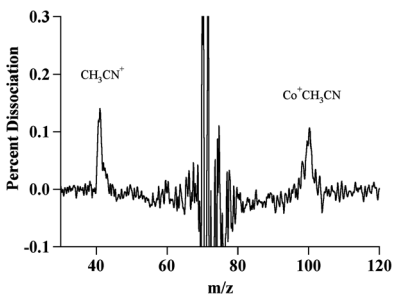

Fig. 2 Difference mass spectrum of $Co^{2+}(CH_3CN)_2$ at 532 nm. Photodissociation occurs by electron transfer, producing CH_3CN^{+} and $Co^{+}(CH_3CN)$. Due to the very low photodissociation yield, the difference spectrum is very noisy near the parent mass and has been cropped.

Our photofragmentation studies of $M^{2+}(CH_3CN)_n$ show similar dissociation pathways to studies conducted using collision-induced dissociation (CID). Kohler and Leary have compared the CID of divalent cations, $M^{2+}(CH_3CN)_n$, of alkaline earth metals Ca and Sr and transition metals Mn and Co.[9,10] For cobalt, clusters with $n \geq 3$ dissociate by solvent loss, as in our studies. Clusters with $n = 1$ dissociate by electron transfer and by heterolytic bond cleavage, forming CH_3^{+}. The dependences of the dissociation pathways of the $n = 2$ clusters on collision energy E_{coll} were examined in detail.[10] Interestingly, each channel dominates over a specific collision energy range. At $E_{coll} < 5$ eV the most likely pathway is proton transfer; ligand loss becomes the major pathway at 10 eV and heterolytic bond cleavage is favored at 20 eV. Collision energies above 30 eV lead to electron transfer, producing CH_3CN^{+} and bare M^{+}, presumably due to subsequent dissociation of $M^{+}(CH_3CN)$. Shvartsburg *et al.* have systematically looked at the CID fragmentation pathways for $M^{2+}(CH_3CN)_n$ for M = Be, Mg, Ca, Sr, Ba, Zn, Cd, Mn, Fe, Co, Ni and Cu[18] and for $M^{3+}(CH_3CN)_n$ complexes of lanthanides.[35] For Co and Ni, the $n = 3$ clusters primarily lose acetonitrile, while $n = 2$ dissociate by solvent loss, heterolytic bond cleavage to CH_3^{+}, electron transfer and proton transfer. The relative amounts of electron transfer and proton transfer depend on the metal and collision energy. In our study of photolysis of $Co^{2+}(CH_3CN)_2$ and $Ni^{2+}(CH_3CN)_2$ only electron transfer is observed. Our calculations show that solvent loss requires ~4.4 eV, about twice the available photon energy. The barrier to proton transfer is also likely well above the photon energy.

B. Mixed M^{2+} clusters with acetonitrile and water

Photodissociation of $Co^{2+}(CH_3CN)_4$ leads to solvent loss, while photodissociation of $Co^{2+}(H_2O)_4$ occurs by proton transfer (charge reduction). Studies of mixed clusters

$Co^{2+}(CH_3CN)_n(H_2O)_m$ with $n + m = 4$ provide an opportunity to observe the evolution of the dissociation pathways as a strong, aprotic solvent is progressively replaced by a weaker, protic solvent. When one acetonitrile is replaced by water to form $Co^{2+}(CH_3CN)_3(H_2O)$, dissociation occurs exclusively by loss of water, which implies that acetonitrile is more strongly bound to Co^{2+} than water. This is due to its higher dipole moment and polarizability. The calculations support this hypothesis, as loss of water requires $\sim$1.0 eV less energy.

The photodissociation of $Co^{2+}(CH_3CN)_2(H_2O)_2$ is also dominated by solvent water loss, but two other minor products are observed: loss of $2H_2O$ and proton transfer (as shown in Fig. 3). The same pathways are observed for $Ni^{2+}(CH_3CN)_2(H_2O)_2$, although the branching ratio for proton transfer is about 3 times higher than for the cobalt complex. The two fragments resulting from proton transfer are protonated acetonitrile and the complementary singly charged metal hydroxide. Proton transfer was further studied by using deuterated acetonitrile to see if the proton comes from acetonitrile or water. The fragment observed is $H^+(CD_3CN)$ rather than $D^+(CD_3CN)$, indicating that water is the proton donor, as expected. We were not able to study $M^{2+}(CH_3CN)(H_2O)_3$ due to our inability to produce a stable parent. Previous studies in our lab have shown that $Co^{2+}(H_2O)_4$ dissociates *via* proton transfer. From our results it is evident that an increase in the number of water molecules in the cluster skews the dissociation dynamics towards the proton transfer channel. There are two reasons for this. One is that three acetonitrile solvent molecules are much better able to stabilize M^{2+} than three waters. The second reason is that protic water is a much better proton donor than aprotic acetonitrile.

Calculations for the four-coordinate clusters agree that the preferred dissociation pathway is simple solvent loss. Water loss is energetically favored by $\sim$1 eV compared to acetonitrile loss. The other major dissociation pathway is proton transfer. Production of two singly charged fragments results in a low energy pathway. However, the activation barrier leading towards the fragments can be quite high, and the transition state for proton transfer is tighter than that for solvent loss, which can make this channel kinetically disfavored in many cases where it is thermodynamically favored. This will be discussed in more detail below.

Photodissociation of the mixed three-coordinate cluster, $Co^{2+}(CH_3CN)_2(H_2O)$, produces solvent water loss (major) and proton transfer (minor), as shown in Fig. 4. Unlike in the four-coordinate clusters, acetonitrile loss is not observed. Calculations predict that loss of acetonitrile requires 1.4 eV more energy than water loss. The minor pathway is proton transfer, which results in protonated acetonitrile and the complementary metal hydroxide. The proton transfer pathway is exothermic by 0.53 eV, in contrast to the endothermic simple solvent losses. However, it does not produce an abundance of fragments because this process has a calculated activation barrier of 1.06 eV at the B3LYP/6-311++G(2df,2pd) level, and the transition state is tighter than that for simple solvent loss. As for smaller mixed clusters, we did not produce sufficient amounts of $Co^{2+}(CH_3CN)(H_2O)_2$ to study. This is likely because the barrier to proton transfer for this molecule is so low that it dissociates in the ion source.

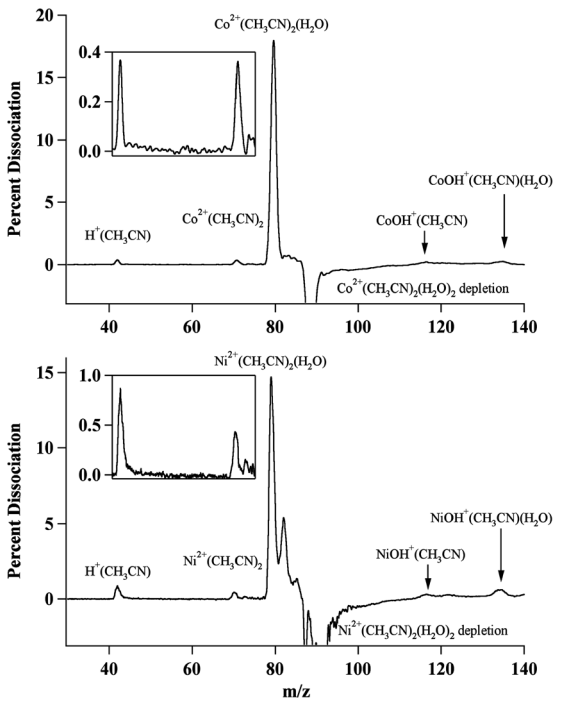

Fig. 3 Difference mass spectra of $Co^{2+}(CH_3CN)_2(H_2O)_2$ (top) and $Ni^{2+}(CH_3CN)_2(H_2O)_2$ (bottom) at 532 nm. The fragmentation pathways are H_2O loss (major), loss of $2H_2O$ (minor) and proton transfer (minor). The insets magnify the low mass range. The nickel complex shows substantially higher branching to proton transfer than the cobalt complex.

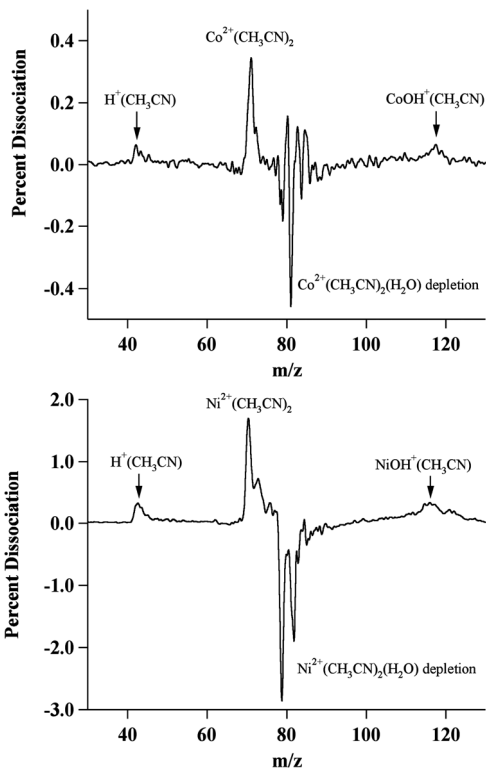

Fig. 4 Difference mass spectra of $Co^{2+}(CH_3CN)_2(H_2O)$ (top) and $Ni^{2+}(CH_3CN)_2(H_2O)$ (bottom) at 532 nm. The fragmentation pathways are water loss (major) and proton transfer (minor).

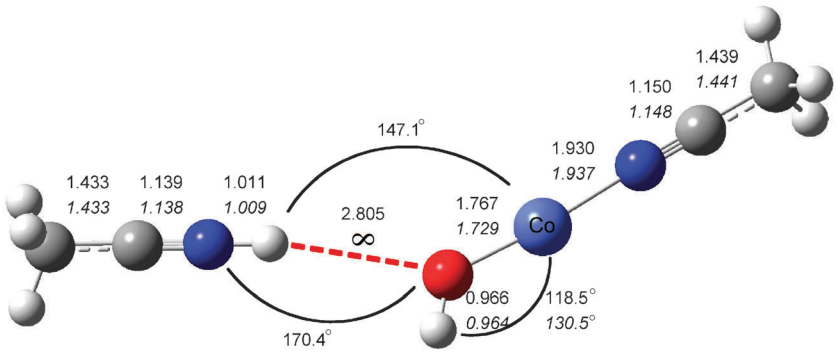

Fig. 5 Calculated, B3LYP/6-311++G(2df,2pd), geometry of the transition state of $Co^{2+}(CH_3CN)_2(H_2O)$ before dissociation to $CoOH^+(CH_3CN)$ + $H^+(CH_3CN)$. The upper number is the geometry for the transition state; the lower number, in italics, is the corresponding parameter in the separated and fully relaxed products. Distances are in Å. In the transition state, the major charge centers, Co^{2+}, OH^-, and H^+ are in an almost linear arrangement. This salt-bridge transition state minimizes the Coulomb barrier for the reaction.

Detailed calculations by Beyer *et al.*[36,37] show that when small $M^{2+}(H_2O)_n$ clusters dissociate *via* proton transfer, the transition state adopts a salt-bridge arrangement M^{2+}–OH^-–H_3O^+. This lowers the Coulomb barrier to fragments. The $Co^{2+}(H_2O)_4$ system[37] is the most similar to the present studies. $Co^{2+}(H_2O)_4$ lies 0.22 eV above the proton transfer products H_3O^+ + $CoOH^+(H_2O)_2$. However, $Co^{2+}(H_2O)_4$ is kinetically stable because proton transfer has a 1.5 eV barrier. If we consider the thermodynamics of $Co^{2+}(CH_3CN)_2(H_2O)$, our calculations show that proton transfer is exothermic by 0.53 eV in the absence of a photon. However, the $Co^{2+}(CH_3CN)_2(H_2O)$ attractive potential and the $CoOH^+(CH_3CN)$–$H^+(CH_3CN)$ repulsive potentials are separated by a significant barrier, thus allowing us to observe thermodynamically unstable $Co^{2+}(CH_3CN)_2(H_2O)$. Following photoexcitation of $Co^{2+}(CH_3CN)_2(H_2O)$ one of the CH_3CN ligands moves to the second solvent shell, with a hydrogen bond from the nitrogen to the inner-shell H_2O. This proton is then transferred. The transition state for proton transfer in $Co^{2+}(CH_3CN)_2$-(H_2O) is also calculated to have a salt-bridge structure $(CH_3CN)Co^{2+}$–OH^-–$H^+(NCCH_3)$, as shown in Fig. 5. It lies 1.06 eV above $Co^{2+}(CH_3CN)_2(H_2O)$. The transition state occurs at long OH^-–H^+ distance (2.805 Å) and the geometries of the $(CH_3CN)CoOH^+$ and $H^+(NCCH_3)$ moieties at the transition state are very similar to those of the separated products, with the only significant change in the Co–O–H angle. The salt-bridge transition state is thus a late transition state. Despite this, the transition state is 1.59 eV above separated products, due to the long-range Coulomb repulsion between the charged products. The dissociation coordinate, which has a calculated frequency of 46*i* cm^{-1}, consists almost entirely of the $(CH_3CN)CoOH^+$–$H^+(NCCH_3)$ stretch. This transition state is very similar to that calculated[37] for proton transfer dissociation of $Co^{2+}(H_2O)_4$ *via* $(H_2O)_2Co^{2+}$ –OH^-–H_3O^+, which also occurs at long OH^-–H^+ distance (3.175 Å) and with the major charge centers (Co^{2+}, OH^- and H^+) nearly collinear (150.7°) to minimize Coulomb repulsion. One significant difference between the photodissociation dynamics of $Co^{2+}(CH_3CN)_2(H_2O)$ and $Co^{2+}(H_2O)_4$ is in the experimentally observed kinetic energy release (KER) in the proton transfer products. In $Co^{2+}(H_2O)_4$ the KER is 110 ± 20 kJ mol^{-1}, which leads to significant broadening of the fragment time-of-flight profile.[7,37] In the present studies, little broadening is observed, indicating much smaller KER. This is likely because more of the available energy goes into vibrational excitation of the products. This is facilitated by the greater number of vibrations, particularly at low frequency, of CH_3CN as compared to H_2O.

There have been few previous studies of solvation of multiply charged metal ions by mixed solvents. Seto and Stone studied CID of $Cu^{2+}(CH_3CN)_n$, n = 2–4 and $Cu^{2+}(CH_3CN)_2(H_2O)$ at 20 eV collision energy.[11] The mixed cluster mostly loses water; loss of acetonitrile and both acetonitrile and water are minor channels. Stace and co-workers have looked at Mn^{2+} solvation by mixtures of water and methanol.[31] The ionization energy and dipole moment of methanol are slightly less than those of water, but its polarizability is twice as large as that of water. Methanol is found to bind metal dications more strongly than water, as shown by the observation that for mixed methanol/water clusters of Mn^{2+}, the first solvent shell primarily consists of methanol.[31] In the smaller water/acetonitrile clusters we study, we believe that all the solvent molecules are attached directly to the metal ion, but photoexcitation primarily leads to loss of the more weakly bound water molecules.

C. Photodissociation yield

The relative 532 nm photodissociation yields for the clusters studied are summarized in Table 2. Compared to the cobalt clusters, nickel clusters show lower yield for four-coordinate clusters; significantly higher yield for three-coordinate clusters; and comparable yields for two-coordinate clusters. Given that the absorption spectra of Ni(II) and Co(II) in solution are quite different, we expect the absorption spectra of $Ni^{2+}(CH_3CN)_n(H_2O)_m$ and $Co^{2+}(CH_3CN)_n(H_2O)_m$ to be different as well. The photodissociation yield reflects the differences in absorption cross section and in photodissociation quantum yield that are characteristic to each metal.

It is clear that the four-coordinate Co^{2+} clusters dissociate more readily than those of Ni^{2+}. For example, the photodissociation yield of $Co^{2+}(CH_3CN)_4$ at 532 nm is almost an order of magnitude larger than that of the corresponding nickel cluster. The calculated energy for acetonitrile loss from the nickel cluster is 2.14 eV, which is 0.07 eV lower than for the

Table 2 Relative photodissociation yields for $Co^{2+}(CH_3CN)_n(H_2O)_m$ and $Ni^{2+}(CH_3CN)_n(H_2O)_m$ at 532 nm

Coordination number	Cluster	Photodissociation yield for Co^{2+}	Photodissociation yield for Ni^{2+}
Four	$M^{2+}(CH_3CN)_4$	2.1	0.28
	$M^{2+}(CH_3CN)_3(H_2O)$	2.5	0.74
	$M^{2+}(CH_3CN)_2(H_2O)_2$	1.7	0.46
Three	$M^{2+}(CH_3CN)_3$	0.07	0.46
	$M^{2+}(CH_3CN)_2(H_2O)$	0.15	0.78
Two	$M^{2+}(CH_3CN)_2$	0.08	0.09

cobalt cluster. This suggests that the difference in photodissociation yield is not due to photodissociation quantum yield, but rather is because the nickel clusters absorb much more weakly in the region of the visible targeted in this study (532–660 nm). Both metals show simple solvent loss as the major dissociation pathway for all four-coordinate clusters but differ in the minor dissociation pathways. For example, for the $M^{2+}(CH_3CN)_2(H_2O)_2$ clusters, loss of two H_2O and proton transfer occur in a 1 : 1 ratio for cobalt and in a 1 : 3 ratio for nickel (Fig. 3).

Although the photodissociation pathways are similar for the three-coordinate clusters of nickel and cobalt, the yields show significant differences. The three-coordinate cobalt clusters show very low yields when compared to nickel or the four-coordinate clusters. This appears to primarily be due to the difference in absorption, as the calculated solvent binding energies for the cobalt and nickel clusters are quite similar. Also, although the solvent binding energy in $Co^{2+}(CH_3CN)_3$ is calculated to be above the 2.33 eV photon energy, water loss from $Co^{2+}(CH_3CN)_2(H_2O)$ only requires 1.92 eV, yet the photodissociation yields differ by only about a factor of two. As with the four-coordinate mixed clusters, $Ni^{2+}(CH_3CN)_2(H_2O)$ shows higher branching for proton transfer than the cobalt cluster.

The wavelength dependence of the photodissociation yield was examined from 532 to 660 nm. Since these molecules are quite large and are at thermal energies, the absorption peaks are broad, and hence the wavelength dependence of the photodissociation is weak. The wavelength at which maximum photodissociation is observed, λ_{max}, depends on the coordination number, solvent and metal ion. Our earlier studies conclude that the four-coordinate clusters $M^{2+}(H_2O)_4$ for M = Co and Ni are tetrahedral[6,7] and that these absorptions are red-shifted from spectra in solution.[38] The calculations also predict tetrahedral geometries for $Co^{2+}(CH_3CN)_4$ and $Ni^{2+}(CH_3CN)_4$. Tetrahedral complexes absorb more strongly than square planar due to a lack of an inversion center. The $Co^{2+}(CH_3CN)_4$ complex shows maximum dissociation near 630 nm. Increasing the number of water molecules shifts λ_{max} towards 610 nm. Previous studies in our lab have shown that $Co^{2+}(H_2O)_4$ has $\lambda_{max} \approx 585$ nm with a shoulder extending to 518 nm.[7] Thus, substitution of acetonitrile for water consistently shifts λ_{max} to longer wavelength. The photodissociation spectrum of four-coordinate clusters of nickel is very broad. As the number of acetonitrile molecules increases, λ_{max} moves towards $\sim$590 nm, a small blue shift compared to homogeneous water clusters which have $\lambda_{max} \approx 605$ nm.[6]

Conclusions

Photodissociation of gas-phase complexes of Co^{2+} and Ni^{2+} solvated by acetonitrile and water $M^{2+}(CH_3CN)_n(H_2O)_m$ was studied in the visible and near-UV region of the spectrum. The photodissociation yield, products and their branching ratios depend on the metal, cluster size and composition. Dissociation occurs by simple solvent loss for $n = 3$ and 4 clusters, as was previously observed for $M^{2+}(H_2O)_n$ and $M^{2+}(CH_3OH)_n$ clusters, where solvent loss dominates for $n > 4$.[6–8] Also, for mixed solvent clusters, the more weakly bound solvent is more likely to cleave the electrostatic bond with the metal dication, leading to preferential loss of water. The smallest clusters we could produce with water and methanol had $n = 4$. Acetonitrile stabilizes Co^{2+} and Ni^{2+} better than water, so we are able to produce mixed three-coordinate clusters and pure two-coordinate clusters with acetonitrile.

Another interesting dissociation pathway observed is proton transfer. Proton transfer is only observed when there is at least one water molecule present in the cluster, and is enhanced for smaller clusters and those with a larger water : acetonitrile ratio. Protic solvents like water favor proton transfer, and this is the major dissociation pathway for small clusters. Small acetonitrile clusters also dissociate *via* electron transfer. This is the dominant dissociation pathway for two-coordinate clusters of both metals and is a minor pathway for three-coordinate clusters of nickel.

Nickel dications solvated by acetonitrile and water generally show the same dissociation pathways as the analogous cobalt clusters, with two exceptions. One is that proton transfer is more favored in nickel clusters such as $M^{2+}(CH_3CN)_2(H_2O)_2$. The second is that three-coordinate and four-coordinate Ni^{2+} clusters show similar photodissociation yields, while three-coordinate Co^{2+} clusters have a much lower photodissociation yield than the four-coordinate clusters.

Acknowledgements

Financial support from the National Science Foundation under awards CHE-0608446 and CHE-0911225 is gratefully acknowledged.

References

1 R. B. Metz, *Int. J. Mass Spectrom.*, 2004, **235**, 131.
2 M. K. Beyer, *Mass Spectrom. Rev.*, 2007, **26**, 517.
3 H. Cox and A. J. Stace, *Int. Rev. Phys. Chem.*, 2010, **29**, 555.
4 A. T. Blades, P. Jayaweera, M. G. Ikonomou and P. Kebarle, *J. Chem. Phys.*, 1990, **92**, 5900.
5 A. T. Blades, P. Jayaweera, M. G. Ikonomou and P. Kebarle, *Int. J. Mass Spectrom. Ion Processes*, 1990, **102**, 251.
6 C. J. Thompson, J. Husband, F. Aguirre and R. B. Metz, *J. Phys. Chem. A*, 2000, **104**, 8155.
7 K. P. Faherty, C. J. Thompson, F. Aguirre, J. Michne and R. B. Metz, *J. Phys. Chem. A*, 2001, **105**, 10054.
8 C. J. Thompson, K. P. Faherty, K. L. Stringer and R. B. Metz, *Phys. Chem. Chem. Phys.*, 2005, **7**, 814.

9 M. Kohler and J. A. Leary, *Int. J. Mass Spectrom. Ion Processes*, 1997, **162**, 17.
10 M. Kohler and J. A. Leary, *J. Am. Soc. Mass Spectrom.*, 1997, **8**, 1124.
11 C. Seto and J. A. Stone, *Int. J. Mass Spectrom. Ion Processes*, 1998, **175**, 263.
12 N. Walker, M. P. Dobson, R. R. Wright, P. E. Barran, J. N. Murrell and A. J. Stace, *J. Am. Chem. Soc.*, 2000, **122**, 11138.
13 R. R. Wright, N. R. Walker, S. Firth and A. J. Stace, *J. Phys. Chem. A*, 2001, **105**, 54.
14 N. R. Walker, R. R. Wright and A. J. Stace, *J. Am. Chem. Soc.*, 1999, **121**, 4837.
15 N. R. Walker, R. R. Wright, P. E. Barran, J. N. Murrell and A. J. Stace, *J. Am. Chem. Soc.*, 2001, **123**, 4223.
16 B. J. Duncombe, L. Puskar, B. H. Wu and A. J. Stace, *Can. J. Chem.*, 2005, **83**, 1994.
17 N. R. Walker, R. R. Wright, A. J. Stace and C. A. Woodward, *Int. J. Mass Spectrom.*, 1999, **188**, 113.
18 A. A. Shvartsburg, J. G. Wilkes, J. O. Lay and K. W. M. Siu, *Chem. Phys. Lett.*, 2001, **350**, 216.
19 C. Y. Xiao, K. Walker, F. Hagelberg and A. M. El-Nahas, *Int. J. Mass Spectrom.*, 2004, **233**, 87.
20 J. Guan, L. Puskar, R. O. Esplugas, H. Cox and A. J. Stace, *J. Chem. Phys.*, 2007, **127**, 064311.
21 T. G. Spence, T. D. Burns, G. B. Guckenberger and L. A. Posey, *J. Phys. Chem. A*, 1997, **101**, 1081.
22 T. G. Spence, B. T. Trotter, T. D. Burns and L. A. Posey, *J. Phys. Chem. A*, 1998, **102**, 6101.
23 T. G. Spence, B. T. Trotter and L. A. Posey, *J. Phys. Chem. A*, 1998, **102**, 7779.
24 P. D. Carnegie, B. Bandyopadhyay and M. A. Duncan, *J. Phys. Chem. A*, 2008, **112**, 6237.
25 P. D. Carnegie, B. Bandyopadhyay and M. A. Duncan, *J. Chem. Phys.*, 2011, **134**, 014302.
26 M. F. Bush, J. T. O'Brien, J. S. Prell, C.-C. Wu, R. J. Saykally and E. R. Williams, *J. Am. Chem. Soc.*, 2009, **131**, 13270.
27 M. F. Bush, R. J. Saykally and E. R. Williams, *ChemPhysChem*, 2007, **8**, 2245.
28 M. F. Bush, R. J. Saykally and E. R. Williams, *J. Am. Chem. Soc.*, 2008, **130**, 15482.
29 J. T. O'Brien and E. R. Williams, *J. Phys. Chem. A*, 2008, **112**, 5893.
30 T. E. Cooper, J. T. O'Brien, E. R. Williams and P. B. Armentrout, *J. Phys. Chem. A*, 2010, **114**, 12646.
31 B. J. Duncombe, J. O. S. Ryden, L. Puskar, H. Cox and A. J. Stace, *J. Am. Soc. Mass Spectrom.*, 2008, **19**, 520.
32 O. M. Cabarcos, C. J. Weinheimer and J. M. Lisy, *J. Chem. Phys.*, 1999, **110**, 8429.
33 T. Him, A. V. Tolmachev, R. Harkewicz, D. C. Prior, G. Anderson, H. R. Udseth, R. D. Smith, T. H. Bailey, S. Rakov and J. H. Futrell, *Anal. Chem.*, 2000, **72**, 2247.
34 M. J. Frisch, G. W. Trucks, H. B. Schlegel, G. E. Scuseria, M. A. Robb, J. R. Cheeseman, J. A. Montgomery Jr., T. Vreven, K. N. Kudin, J. C. Burant, J. M. Millam, S. S. Iyengar, J. Tomasi, V. Barone, B. Mennucci, M. Cossi, G. Scalmani, N. Rega, G. A. Petersson, H. Nakatsuji, M. Hada, M. Ehara, K. Toyota, R. Fukuda, J. Hasegawa, M. Ishida, T. Nakajima, Y. Honda, O. Kitao, H. Nakai, M. Klene, X. Li, J. E. Knox, H. P. Hratchian, J. B. Cross, C. Adamo, J. Jaramillo, R. Gomperts, R. E. Stratmann, O. Yazyev, A. J. Austin, R. Cammi, C. Pomelli, J. W. Ochterski, P. Y. Ayala, K. Morokuma, G. A. Voth, P. Salvador, J. J. Dannenberg, V. G. Zakrzewski, S. Dapprich, A. D. Daniels, M. C. Strain, O. Farkas, D. K. Malick, A. D. Rabuck, K. Raghavachari, J. B. Foresman, J. V. Ortiz, Q. Cui, A. G. Baboul, S. Clifford, J. Cioslowski, B. B. Stefanov, G. Liu, A. Liashenko, P. Piskorz, I. Komaromi, R. L. Martin, D. J. Fox, T. Keith, M. A. Al-Laham, C. Y. Peng, A. Nanayakkara, M. Challacombe, P. M. W. Gill, B. Johnson, W. Chen, M. W. Wong, C. Gonzalez and J. A. Pople, Gaussian, Inc., Wallingford, CT, Pittsburgh, PA, 2004.
35 A. A. Shvartsburg, *Chem. Phys. Lett.*, 2002, **360**, 479.
36 M. K. Beyer, E. R. Williams and V. E. Bondybey, *J. Am. Chem. Soc.*, 1999, **121**, 1565.
37 M. K. Beyer and R. B. Metz, *J. Phys. Chem. A*, 2003, **107**, 1760.
38 T. W. Swaddle and L. Fabes, *Can. J. Chem.*, 1980, **58**, 1418.